



Stimulation of σ_1 -receptor restores abnormal mitochondrial Ca^{2+} mobilization and ATP production following cardiac hypertrophy

Hideaki Tagashira^a, Chen Zhang^b, Ying-mei Lu^c, Hideyuki Hasegawa^d, Hiroshi Kanai^e, Feng Han^f, Kohji Fukunaga^{a,*}

^a Department of Pharmacology, Graduate School of Pharmaceutical Sciences, Tohoku University, 6-3 Aramaki-Aoba, Aoba-ku, Sendai, Japan

^b Department of Pharmacy, College of Pharmaceutical Sciences, Zhejiang University, Hangzhou, Zhejiang 31005, PR China

^c Department of Neurobiology, Zhejiang University School of Medicine, 388 Yu Hang Tang Road, Hangzhou 310058, PR China

^d Department of Electrical Engineering, Graduate School of Biomedical Engineering, Tohoku University, 6-6 Aramaki-Aoba, Aoba-ku, Sendai, Japan

^e Department of Electrical Engineering, Graduate School of Engineering, Tohoku University, 6-6 Aramaki-Aoba, Aoba-ku, Sendai, Japan

^f Institute of Pharmacology, Toxicology and Biochemical Pharmaceutics, Zhejiang University, Hangzhou, Zhejiang 31005, PR China



ARTICLE INFO

Article history:

Received 2 October 2012

Received in revised form 21 December 2012

Accepted 26 December 2012

Available online 6 January 2013

Keywords:

ATP
Calcium signaling
ATP production
Mitochondria
Sigma receptor

ABSTRACT

Background: We previously reported that the σ_1 -receptor (σ_1R) is down-regulated following cardiac hypertrophy and dysfunction in transverse aortic constriction (TAC) mice. Here we address how σ_1R stimulation with the selective σ_1R agonist SA4503 restores hypertrophy-induced cardiac dysfunction through σ_1R localized in the sarcoplasmic reticulum (SR).

Methods: We first confirmed anti-hypertrophic effects of SA4503 (0.1–1 μM) in cultured cardiomyocytes exposed to angiotensin II (Ang II). Then, to confirm the ameliorative effects of σ_1R stimulation *in vivo*, we administered SA4503 (1.0 mg/kg) and the σ_1R antagonist NE-100 (1.0 mg/kg) orally to TAC mice for 4 weeks (once daily).

Results: σ_1R stimulation with SA4503 significantly inhibited Ang II-induced cardiomyocyte hypertrophy. Ang II exposure for 72 h impaired phenylephrine (PE)-induced Ca^{2+} mobilization from the SR into both the cytosol and mitochondria. Treatment of cardiomyocytes with SA4503 largely restored PE-induced Ca^{2+} mobilization into mitochondria. Exposure of cardiomyocytes to Ang II for 72 h decreased basal ATP content and PE-induced ATP production concomitant with reduced mitochondrial size, while SA4503 treatment completely restored ATP production and mitochondrial size. Pretreatment with NE-100 or siRNA abolished these effects. Chronic SA4503 administration also significantly attenuated myocardial hypertrophy and restored ATP production in TAC mice. SA4503 administration also decreased hypertrophy-induced impairments in LV contractile function.

Conclusions: σ_1R stimulation with the specific agonist SA4503 ameliorates cardiac hypertrophy and dysfunction by restoring both mitochondrial Ca^{2+} mobilization and ATP production via σ_1R stimulation.

General significance: Our observations suggest that σ_1R stimulation represents a new therapeutic strategy to rescue the heart from hypertrophic dysfunction.

© 2013 Elsevier B.V. All rights reserved.

1. Introduction

Administration of selective serotonin reuptake inhibitors (SSRIs), which are used to treat depression, to patients who have undergone myocardial infarction reportedly reduces post-MI morbidity and mortality [1]. Although the mechanism underlying that effect remains unclear, it is known that SSRIs such as sertraline [2] and fluvoxamine [3], in addition to acting on serotonin transporters, bind with high

affinity to the σ_1 -receptor (σ_1R), suggesting that cardioprotective activity is mediated by σ_1R stimulation. We recently confirmed that the σ_1R is more highly expressed in neonatal rat cardiomyocytes and rat heart than it is in brain and other peripheral tissues [4,5]. We also observed reduction in σ_1R levels in the left ventricle accompanying progression of left ventricular hypertrophy in transverse aortic constriction (TAC) mice and a significant positive correlation between σ_1R expression and impaired LV fractional shortening [6]. σ_1R stimulation with fluvoxamine rescues impaired LV fractional shortening and reduces hypertrophy in the TAC mice [6]. Furthermore treatment with a different σ_1R agonist, the neurosteroid dehydroepiandrosterone (DHEA), significantly antagonizes pressure overload (PO)-induced decreases in σ_1R expression in rat heart [7,8] and thoracic arteries [9,10]. On the other hand, Ito et al. [11] reported that suppression of sympathetic nerve activation by an σ_1R agonist in brain improves impaired LV fractional shortening in a pressure overload- and high-salt diet-induced heart

Abbreviations: SA4503, 1-(3,4-dimethoxyphenethyl)-4-(3-phenylpropyl)piperazine dihydrochloride; NE-100, N,N-dipropyl-2-[4-methoxy-3-(2-phenylethoxy) phenyl]-ethylamine monohydrochloride; SR, sarcoplasmic reticulum; TAC, transverse aortic constriction; IP3R, inositol trisphosphate receptors; ATP, adenosine triphosphate; MAM, mitochondria-associated ER membrane; TCA cycle, tricarboxylic acid cycle; PE, phenylephrine

* Corresponding author. Tel.: +81 22 795 6837; fax: +81 22 795 6835.

E-mail address: kfukunaga@m.tohoku.ac.jp (K. Fukunaga).

failure mouse model. This finding suggests that fluvoxamine indirectly blunts impaired LV fractional shortening in this model. We previously asked whether fluvoxamine directly elicits an anti-hypertrophic effect on cultured cardiomyocytes and found that fluvoxamine reduced angiotensin II (Ang II)-induced hypertrophy by stimulating the σ_1 R in cardiomyocytes [6]. Indeed, σ_1 R knockdown in cardiomyocytes totally abolished this effect. However, the mechanism underlying the anti-hypertrophic effects of fluvoxamine [6] and DHEA [8] and their effect on intracellular Ca^{2+} regulation remains unclear.

In non-cardiomyocytes, the σ_1 R localizes to the mitochondria-associated ER membrane (MAM) and interacts with the IP_3 receptor (IP_3R), which likely promotes Ca^{2+} transport into mitochondria from the ER [12]. In the IP_3R family, $\text{IP}_3\text{R}2$ is the most prominent isoform expressed in the heart [13,14]. Transgenic mice expressing an IP_3 -chelating protein (IP_3 sponge), which binds free IP_3 with high affinity and inhibits IP_3R function in the heart [15], are resistant to isoproterenol-induced hypertrophy [16]. Taken together, IP_3 -mediated Ca^{2+} release plays an important role in development of cardiac hypertrophy, and σ_1 R agonists likely modulate IP_3 -mediated Ca^{2+} release in cardiomyocytes. However, it is not known how the σ_1 R modulates mitochondrial Ca^{2+} mobilization through $\text{IP}_3\text{R}2$ in cardiomyocytes or whether reducing σ_1 R levels following hypertrophy would alter mitochondrial Ca^{2+} mobilization.

In this study, to determine whether σ_1 R stimulation directly affects IP_3R function in cardiomyocytes, we used the specific, high affinity σ_1 R agonist SA4503 (1-(3,4-dimethoxyphenethyl)-4-(3-phenylpropyl)piperazine dihydrochloride) ($K_i = 4.4$ nM) to define the function of σ_1 R-mediated IP_3R regulation of mitochondrial Ca^{2+} transport into cardiomyocytes in vitro and in vivo. We made the novel observation that SA4503 ameliorates Ang II-induced impairment of SR-mitochondrial Ca^{2+} transport and mitochondrial ATP production via σ_1 R stimulation. We found that enhanced ATP production following SA4503 administration restored cardiac contractile dysfunction in TAC mice. This study suggests that the σ_1 R could be a novel therapeutic target to rescue cardiomyocytes from myocardial infarction.

2. Materials and methods

2.1. Materials

Reagents and antibodies were obtained from the following sources: anti- σ_1 R antibody (Abcam, Cambridge, UK); anti- IP_3 receptor type 2 (American Research Products Inc. Waltham, MA); anti-mitofusin 2 (Sigma, St. Louis, MO); anti-mitofusin 1 (Abcam, Cambridge, UK); anti-voltage-dependent anion channel (VDAC) (Cell Signaling Technology, Beverly, MA); anti-GRP75 (Cell Signaling Technology, Beverly, MA); anti-Cytochrome c (BD Biosciences, San Diego, CA); and anti- β -tubulin antibody (Sigma, St. Louis, MO). The σ_1 R agonist SA4503 was synthesized in the Laboratory of Medicinal Chemistry, Zhejiang University according to the method of Fujimura et al. [17]. The specific σ_1 R antagonist NE-100 (N,N-dipropyl-2-[4-methoxy-3-(2-phenylethoxy)phenyl]-ethylamine monohydrochloride) was generously supplied by Taisho Pharmaceutical Co. Ltd (Ohmiya, Japan). Other reagents were of the highest quality available (Wako Pure Chemicals, Osaka, Japan).

2.2. Animals and operations

All procedures for handling animals complied with the *Guide for Care and Use of Laboratory Animals* and were approved by the Animal Experimentation Committee of Tohoku University Graduate School of Pharmaceutical Sciences. Adult male ICR mice weighing 35 to 40 g were obtained from Nippon SLC (Hamamatsu, Japan). Ten-week-old males were acclimated to the local environment for 1 week, which included housing in polypropylene cages at 23 ± 1 °C in a humidity-controlled environment maintained on a 12-h light/dark schedule (lights on 8:00 AM–8:00 PM). Mice were provided food and water

ad libitum. Transverse aortic constriction (TAC) was performed as previously described [6] on male ICR mice under anesthesia using a mixture of ketamine (100 mg/kg, i.p.) (Daiichi Sankyo Pharmaceutical Co. Ltd, Tokyo, Japan) and xylazine (5 mg/kg, i.p.) (Sigma, St. Louis, MO). Adequate depth of anesthesia was confirmed by a negative toe-pinch reflex. If anesthesia was not sufficient, then a top-up dose of 20% of the initial dose was given.

2.3. Experimental design

ICR mice were randomly separated into six experimental groups: 1) sham ($n = 5$), 2) TAC for 4 weeks ($n = 5$), 3) TAC plus SA4503 (0.1 mg/kg, p.o.) treatment (SA 0.1) ($n = 5$), 4) TAC plus SA4503 (0.3 mg/kg, p.o.) treatment (SA 0.3) ($n = 5$), 5) TAC plus SA4503 (1.0 mg/kg, p.o.) treatment (SA 1.0) ($n = 5$), 6) TAC plus SA4503 (1.0 mg/kg, p.o.) plus NE-100 treatment (1.0 mg/kg, p.o.) (SA 1.0 + NE) ($n = 5$). SA4503 and NE-100 were dissolved in a 0.9% saline solution. Vehicle, SA4503 and NE-100 (1.0 mg/kg) were administered orally for 4 weeks (once daily) using a metal gastric gavage cannula in a volume of 1 ml/100 g of mouse body weight, starting from the onset of aortic banding.

2.4. Echocardiography and measurement of cardiac hypertrophy

Noninvasive echocardiographic measurements were performed as described [6]. Briefly, noninvasive echocardiographic measurements were performed in mice anesthetized with pentobarbital-NaCl/EtOH solution (0.05 g/kg i.p.) using ultrasonic diagnostic equipment (SSD-6500; Aloka, Tokyo, Japan) equipped with a 10-MHz linear array transducer (UST-5545; Aloka). The heart was imaged in the two-dimensional parasternal short-axis view, and an M-mode echocardiogram of the midventricle was recorded at the level of the papillary muscles. Diastolic and systolic LV wall thickness, LV end-diastolic diameter (LVEDD) and LV end-systolic diameter (LVESD) were measured. All measurements were done from leading edge to leading edge according to the American Society of Echocardiography guidelines. The percentage of LV fraction shortening (LV%FS) was calculated as $(\text{LVEDD} - \text{LVESD})/\text{LVEDD} \times 100$. After sacrificing by cervical spine fracture dislocation, the thoracic cavity was opened, and hearts were immediately harvested and weighed.

2.5. Transfection of cultured cardiomyocytes

Neonatal rat ventricular cardiomyocytes were isolated from hearts of 1- to 3-day-old Wistar rats, which had been sacrificed by decapitation, and cardiomyocytes were cultured as described [6]. σ_1 R siRNA (sense, 5'-ACACGTTGGATGGTGGAGTA-3' and anti-sense, 5'-TACTCCACCATC CACGTGT-3') was purchased from Exigen Ltd., Tokyo, Japan. Cultured myocytes were plated on uncoated 90-mm culture dishes on collagen-coated cover glasses. Transfections were performed using 100 nM σ_1 R siRNAs as described [6].

2.6. Morphological analysis and immunocytochemistry of cultured cardiomyocytes

Morphological analysis was performed as described [6]. The surface area of control cells was set at 100% and compared with that of treated cells. For mitochondrial staining, cells were stained for 20 min with 0.02 μM MitoTracker Red CMXRos (Molecular Probes) before fixation. After permeabilization with 0.1% Triton X-100 in PBS, fixed cells were incubated with 1% bovine serum albumin in PBS for 30 min. For immunocytochemistry, cells were incubated 24 h at 4 °C with anti- σ_1 R antibody (1:500) or anti-Cytochrome c antibody (1:500) in PBS containing 1% BSA. After washing, cells were incubated 24 h with Alexa 488 in PBS containing 1% BSA. Immunofluorescent images were

obtained with a confocal laser scanning microscope (TCS SP, Leica Microsystems).

2.7. Western blot analysis and measurement of ATP content

Dissected LV tissue samples were rapidly frozen in liquid nitrogen and stored at -80°C before analysis. In the case of cardiomyocytes, cells were washed with PBS at 4°C and stored at -80°C until immunoblotting analyses were performed as described [18]. For assays, each frozen sample was homogenized as described [6,19]. ATP measurement was performed using an ATP assay kit (Toyo Ink, Tokyo, Japan), according to the manufacturer's protocol. Briefly, frozen samples were homogenized in homogenate buffer (0.25 M sucrose, 10 mM HEPES-NaOH: pH 7.4), and lysates were cleared by centrifugation at 1000 g for 10 min at 4°C . The supernatant was collected, and proteins in the supernatant were solubilized in extraction buffer. After 30 min, luciferin buffer was added to each sample and oxyluciferin was detected using a luminometer (Gene Light 55, Microtec, Funabashi, Japan).

2.8. Measurement of intracellular Ca^{2+}

Neonatal ventricular myocytes were cultured on 0.01% poly-L-lysine (Sigma-Aldrich) coated glass-bottom dishes and maintained in growth medium. After stimulation with 100 nM Ang II for either 48 or 72 h, myocytes were loaded with the Ca^{2+} -sensitive dye Fura-2 acetoxymethyl ester (2.5 μM) for 30 min before measuring Ca^{2+} levels in a chamber on an inverted microscope stage. Cells were perfused with normal Tyrode solution containing 150 mM NaCl, 4 mM KCl, 1 mM MgCl_2 , 2 mM CaCl_2 , 5.6 mM glucose, and 5 mM HEPES at 37°C . When Ca^{2+} fluorescence levels reached a steady state, 10 μM phenylephrine (PE) and 10 mM caffeine were applied for 10 s through a small perfusion pipe. The amplitude of the PE-induced Ca^{2+} transient was used as an index of IP_3R -mediated Ca^{2+} release. The amplitude of the caffeine-induced Ca^{2+} transient served as an index of sarcoplasmic reticulum Ca^{2+} content [20,21]. Changes in PE-induced Ca^{2+} release and caffeine-induced Ca^{2+} release from the sarcoplasmic reticulum were determined using the ratio of fluorescence emission at 530 nm in response to excitation at 340 nm and to that at 380 nm.

2.9. Measurement of mitochondrial Ca^{2+}

Neonatal ventricular myocytes were cultured on 0.01% poly-L-lysine (Sigma-Aldrich) coated glass-bottom dishes and maintained in growth medium. Transfections were performed with ratiometric pericam targeted to the mitochondrial matrix (ratiometric-pericam-mt/pcDNA3), which was a kind gift of Dr. Atsushi Miyawaki of the RIKEN Brain Science Institute (Wako-city, Japan). Briefly, 1 $\mu\text{g}/\mu\text{l}$ ratiometric-pericam-mt/pcDNA3 in 1 μl was added to 199 μl opti-MEM (Invitrogen), and 1 μl Lipofectamine 2000 (Invitrogen) was added to 9 μl opti-MEM. Both solutions were incubated separately at room temperature for 5 min and then mixed and incubated at room temperature for 15 to 20 min. Cells were incubated with 800 μl of opti-MEM to which 200 μl of the ratiometric-pericam-mt/pcDNA3 solution had been added. Cells were then incubated at 37°C in a 5% CO_2 atmosphere for 4 h to initiate transfection. Then, 500 μl DMEM supplemented with 5% FBS was added to each well to maintain cell viability. After 24 h, 100 nM Ang II was added. After stimulation for 48 or 72 h, cells were perfused with normal Tyrode solution at 37°C . When Ca^{2+} fluorescence levels reached a steady state, 10 μM PE was applied for 10 s through a small perfusion pipe. Dual-excitation imaging with ratiometric-pericam-mt required two filters (EX:482/35, DM:506, EM:536/40 and EX:414/46, DM:510, EM:527/20). Changes in PE-induced Ca^{2+} transport from the sarcoplasmic reticulum to mitochondria were determined using the Metafluor Imaging system (Molecular Devices, Sunnyvale, CA).

2.10. Statistical analysis

Values are represented as means \pm standard error of the mean (S.E.M.). Results were evaluated for differences using one-way analysis of variance (ANOVA), followed by multiple comparisons using Scheffe's test. $P < 0.05$ was considered statistically significant.

3. Results

3.1. SA4503 treatment ameliorates Ang II-induced cardiomyocyte hypertrophy

We previously documented that fluvoxamine elicits antihypertrophic effects on Ang II-induced hypertrophy through $\sigma_1\text{R}$ stimulation. We first confirmed the antihypertrophic effect of the selective $\sigma_1\text{R}$ agonist SA4503 on Ang II-induced hypertrophy. Neonatal rat cultured cardiomyocytes were exposed to Ang II for 72 h with or without treatment with SA4503, NE-100 or the selective IP_3R inhibitor xestospongins C for the last 24 h. None of these treatments had an effect on the size of untreated (control) cells; however, the size of Ang II-treated cells significantly increased compared to control cells 72 h after Ang II exposure ($P < 0.01$ vs. control) (Fig. 1A and B). SA4503 treatment inhibited Ang II-induced cell enlargement dose-dependently ($P < 0.01$ vs. Ang II) (Fig. 1A and B). Combined treatment with NE-100 reversed SA4503-mediated inhibition of cardiomyocyte hypertrophy ($P < 0.01$ vs. SA 1.0) (Fig. 1A and B). Interestingly, combined treatment with xestospongins C and SA4503 partially but significantly reversed SA4503-mediated inhibition of cardiomyocyte hypertrophy ($P < 0.01$ vs. SA 1.0) (Fig. 1A and B). These findings suggest that SA4503 directly acts on the cardiac $\sigma_1\text{R}$ to antagonize Ang II-induced cardiomyocyte enlargement, an effect partially mediated by IP_3R stimulation.

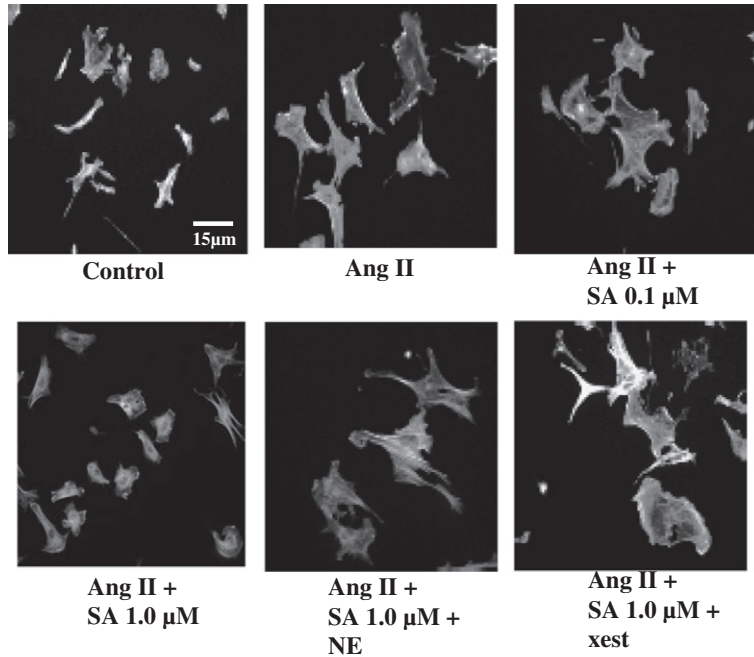
3.2. Effect of SA4503 treatment on PE-induced Ca^{2+} influx into mitochondria and the cytosol

To test our hypothesis that $\sigma_1\text{R}$ stimulation regulates IP_3R -mediated Ca^{2+} mobilization in cardiomyocytes, we examined the effects of SA4503 on PE-induced IP_3R -mediated Ca^{2+} mobilization into mitochondria and the cytosol in Ang II-treated cells. Treatment with SA4503 alone for 24 h had no effect on PE-induced mitochondrial Ca^{2+} mobilization in control cells. At 72 h after treatment, Ang II exposure severely impaired PE-induced mitochondrial Ca^{2+} mobilization compared to effects seen in untreated control cells ($P < 0.01$ vs. control) (Fig. 2A, B and C). SA4503 treatment during the last 24 h significantly restored PE-induced Ca^{2+} mobilization in mitochondria ($P < 0.01$ vs. Ang II) (Fig. 2A, B and C). We also examined the effects of SA4503 on PE-induced IP_3R -mediated Ca^{2+} mobilization into the cytosol. SA4503 treatment alone for 24 h had no effect on PE-induced Ca^{2+} mobilization into the cytosol in control cells. Like mitochondrial Ca^{2+} mobilization, Ang II exposure for 72 h significantly suppressed Ca^{2+} mobilization, and SA4503 treatment partially rescued that effect ($P < 0.01$ vs. control) (Fig. 2D, E and F). These results suggest that SA4503 treatment preferentially rescues IP_3R -mediated mitochondrial Ca^{2+} mobilization but partly rescues IP_3R -mediated Ca^{2+} mobilization into the cytosol.

3.3. Effect of SA4503 treatment on $\sigma_1\text{R}$ expression, its association with mitochondria, and mitochondrial ATP content

Since SA4503 promotes IP_3R -mediated Ca^{2+} mobilization, particularly into mitochondria, we asked whether $\sigma_1\text{R}$ activity governs mitochondrial morphology and functions in ATP production. MitoTracker Red CMXRos detects not only mitochondrial morphology but also mitochondrial membrane potential because of intake of mitochondria in a membrane potential-dependent manner [22]. We first confirmed an association of the $\sigma_1\text{R}$ with mitochondrial membranes in cultured

A



B

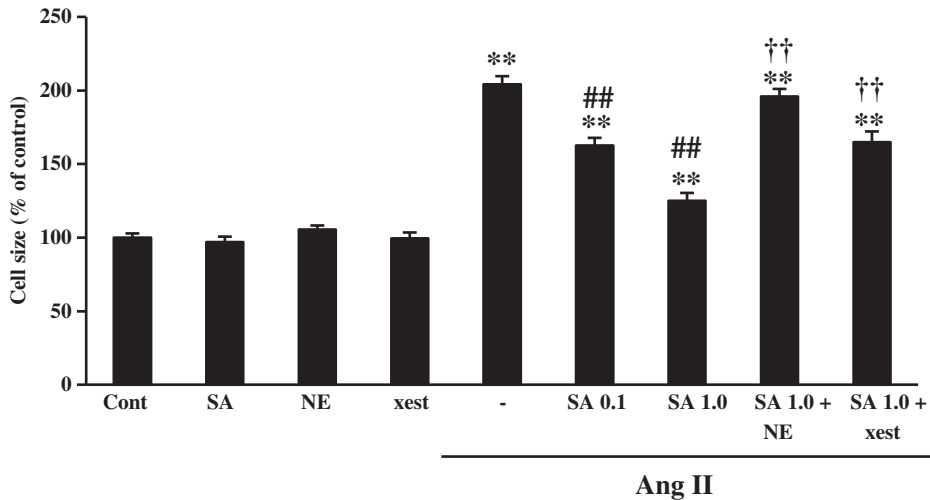


Fig. 1. Effects of SA4503 treatment on Ang II-induced hypertrophy of cultured cardiomyocytes. A, cells were fixed with 4% paraformaldehyde, stained with Rhodamine-conjugated Phalloidin, and processed for fluorescence microscopy. One hundred cells from randomly selected fields were evaluated in each condition for cell size. B, cell size is expressed as a percentage of the relative surface area compared to control cells. Each column represents the mean \pm S.E.M. **, $P < 0.01$ versus the control cells; ##, $P < 0.01$ versus Ang II-treated cells; ††, $P < 0.01$ versus Ang II plus 1 μ M SA4503-treated cells. NE: NE-100 (10 μ M for 24 h). Xest: xestospongine C (1 μ M for 24 h).

cardiomyocytes. In unstimulated control cells, σ_1 R immunoreactivity largely merged with that of a MitoTracker Red (Fig. 3A: Cont). SA4503 alone treatment did not alter such co-localization (Fig. 3A: SA 24 h). After Ang II exposure for 72 h, σ_1 R immunoreactivity largely disappeared from the cytosol, and mitochondrial tracer fluorescence was also slightly reduced (Fig. 3A: Ang II 72 h). Mitochondrial size significantly decreased after Ang II exposure, suggesting either mitochondrial degradation or enhanced mitochondrial fission. Interestingly, SA4503 treatment for the last 24 h of 72 h Ang II exposure rescued reduced σ_1 R immunoreactivity and inhibited mitochondrial fission and/or degradation (Fig. 3A: Ang II 72 + SA 24 h). Finally, NE-100 treatment antagonized the SA4503-induced protective effect on mitochondrial degradation, as shown by increased mitochondrial fission (Fig. 3A: Ang II 72 + NE + SA 24 h). These data suggest that Ang II treatment of cells causes mitochondrial dysfunction and that SA4503 treatment

protects cells from Ang II-induced mitochondrial fission and/or degradation.

We next examined the effects of Ang II and SA4503 treatment on ATP content. SA4503 treatment alone slightly but significantly enhanced ATP content in control cells, but xestospongine C treatment alone had no effect. As expected, Ang II exposure for 72 h significantly decreased ATP content ($P < 0.01$ vs. control), and SA4503 treatment rescued this effect ($P < 0.01$ vs. Ang II) (Fig. 3B). Treatment with NE-100 combined with σ_1 R knockdown by siRNA totally abolished the SA4503 effect ($P < 0.01$ vs. SA) (Fig. 3B). σ_1 R siRNA effectively reduced σ_1 R levels to 30% of control cells, as shown previously [6]. Finally, xestospongine C treatment largely reversed SA4503-mediated increases in ATP content ($P < 0.01$ vs. SA 1.0). Since increased ATP consumption could persist following Ang II exposure, we examined phenylephrine (PE)-induced ATP production, which peaks within

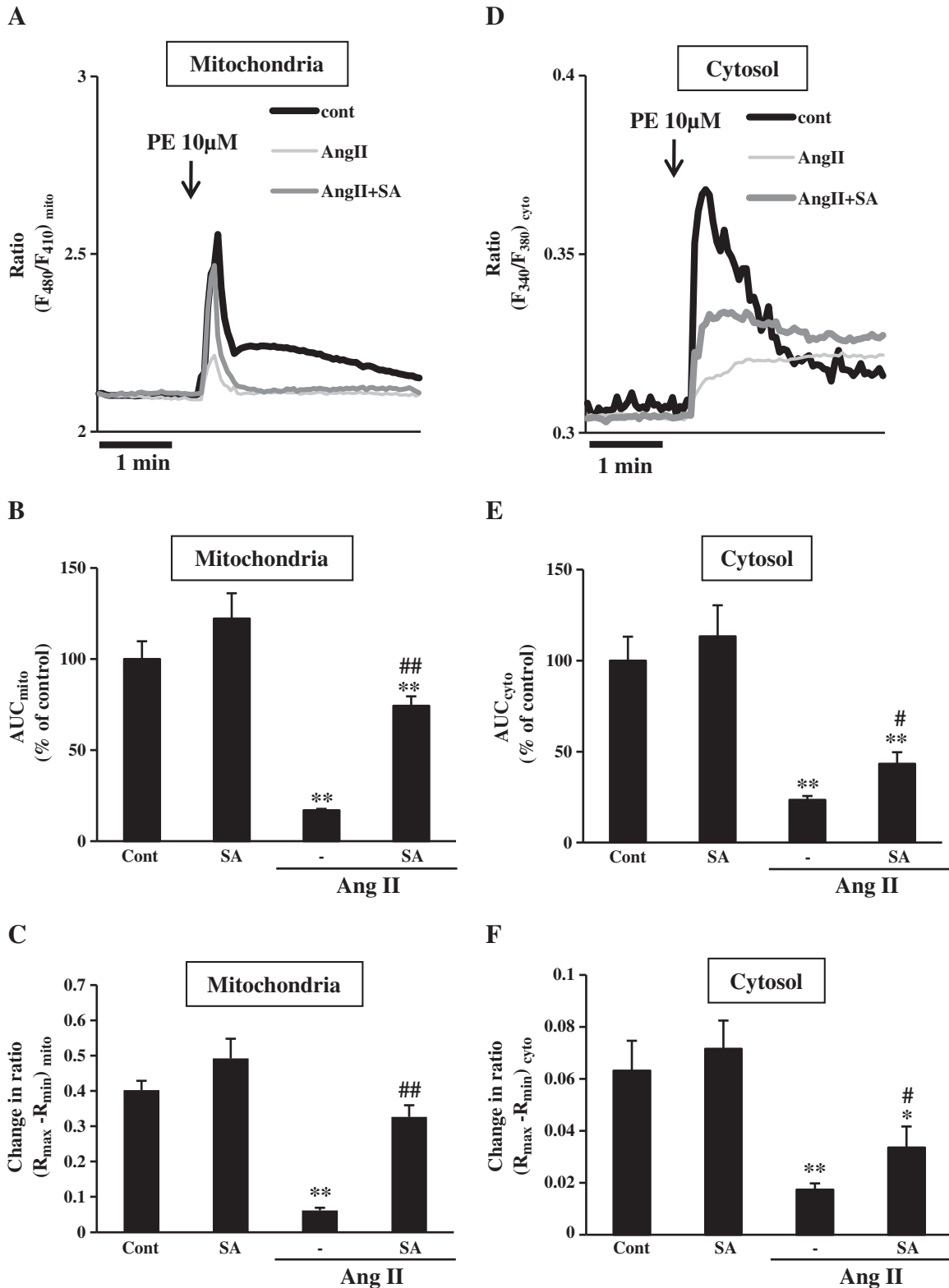
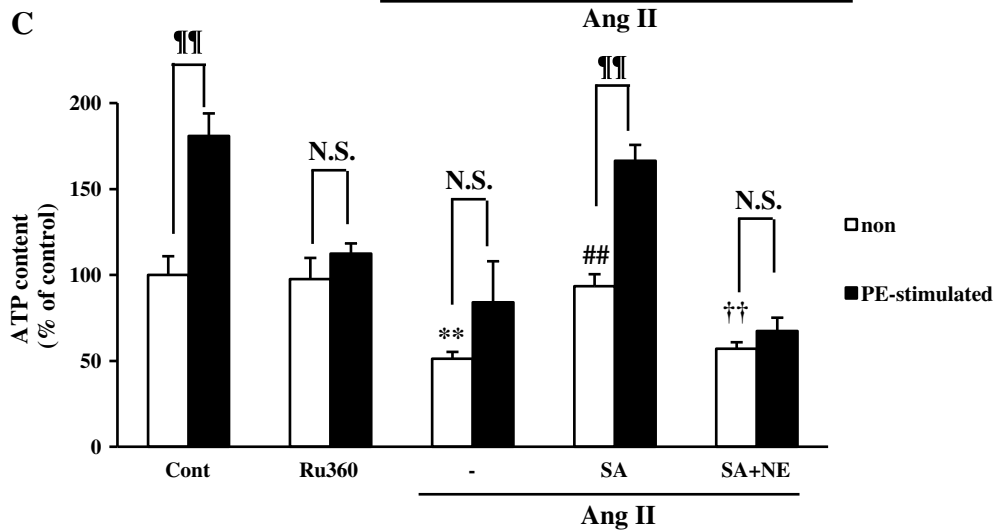
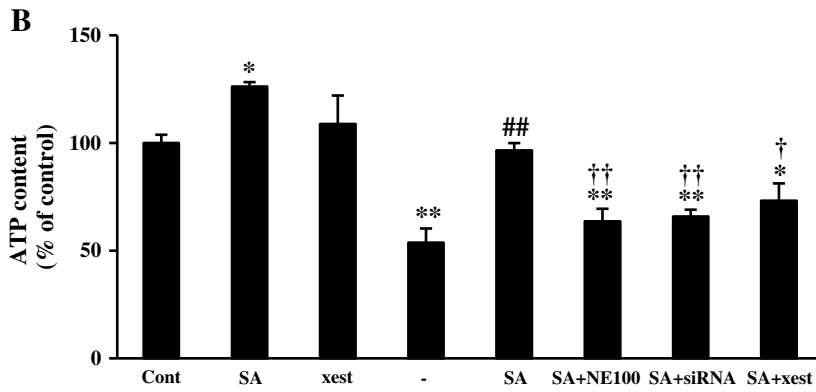
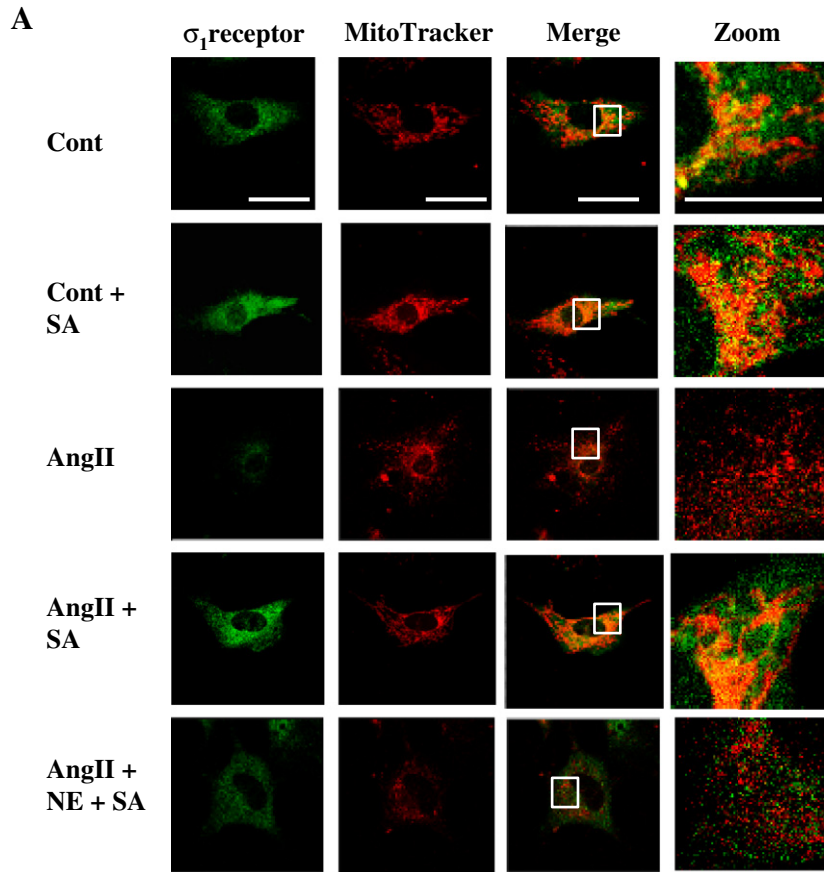


Fig. 2. Effects of SA4503 treatment on PE-induced Ca^{2+} influx into mitochondria and the cytosol. A, time courses of PE-induced Ca^{2+} influx into mitochondria 72 h after 100 nM Ang II treatment with or without SA4503 treatment during the last 24 h. B, area under the curve (AUC) quantification of PE-induced Ca^{2+} influx into mitochondria. C, peak increases in $[\text{Ca}^{2+}]_{\text{mito}}$ induced by 10 μM PE. D, time courses of PE-induced Ca^{2+} release into the cytosol 72 h after 100 nM Ang II treatment with or without SA4503 treatment for the last 24 h. E, AUC quantification of PE-induced Ca^{2+} release into the cytosol. F, peak increases in $[\text{Ca}^{2+}]_{\text{cyto}}$ induced by 10 μM PE. Each group consists of more than 10 cells. Data are expressed as percentages of control cells (mean \pm S.E.M.). *, $P < 0.05$ and **, $P < 0.01$ versus control cells; #, $P < 0.05$ and ##, $P < 0.01$ versus Ang II-treated cells.

15 min of treatment. As shown in Fig. 3C, PE stimulated ATP production up to 180% in naive control cells, whereas PE failed to stimulate ATP production at 72 h after Ang II treatment. When cardiomyocytes

were treated with Ru360, a specific inhibitor of mitochondrial calcium uptake, PE-induced ATP production was completely inhibited (Fig. 3C), suggesting that mitochondrial Ca^{2+} influx functions in



PE-induced ATP production. Notably, ATP content of Ang II-treated cells was markedly decreased compared to naive cells 72 h after Ang II treatment ($P < 0.01$ vs. control) (Fig. 3B and C: white bar), and PE stimulation (Fig. 3C: black bar) failed to increase ATP production. Treatment with SA4503 for the last 24 h of Ang II exposure significantly and completely restored ATP content and PE-induced ATP production. SA4503-mediated rescue of ATP content and PE-induced ATP production was totally abolished in the presence of NE-100 (Fig. 3C). Taken together, our observations strongly suggest that SA4503-mediated increases in ATP content and PE-induced ATP production are mediated by σ_1 R stimulation.

3.4. The effect of sigma-1 receptor stimulation by SA4503 on expression of σ_1 R and ER-mitochondria junctional proteins

We further investigated mitochondrial morphology using another mitochondrial marker protein, Cytochrome c, whose localization is independent of mitochondrial membrane potential. Mitochondrial size decreased after Ang II exposure, suggesting either mitochondrial degradation or enhanced mitochondrial fission. Interestingly, SA4503 treatment for the last 24 h of 72 h Ang II exposure inhibited mitochondrial fission and/or degradation (Fig. 4A: Ang II 72 + SA 24 h). Finally, NE-100 treatment antagonized the SA4503-induced protective effect on mitochondrial degradation, as shown by increased mitochondrial fission (Fig. 4A: Ang II 72 + NE + SA 24 h).

To further define changes in mitochondrial function, we determined expression levels of proteins associated with the SR and mitochondria. Consistent with decreased σ_1 R immunofluorescence observed in Fig. 3A, σ_1 R protein expression levels decreased in Ang II-exposed cells ($P < 0.01$ vs. control) (Fig. 4B, C). SA4503 treatment significantly rescued reduced σ_1 R expression ($P < 0.01$ vs. Ang II) (Fig. 4B, C). Interestingly, although NE-100 treatment abolished SA4503-mediated cardioprotective effects (Fig. 1A), it did not completely abolish SA4503-mediated upregulation of σ_1 R expression (Fig. 4B, C).

Recent studies reveal that specific proteins and chaperones function as ER-mitochondria linkage proteins. For example, mitofusin-2 (Mfn-2) not only connects mitochondria but also bridges the ER with mitochondria and functions in IP₃-induced mitochondrial Ca²⁺ uptake [23]. Moreover, Szabadkai et al. report that glucose-regulated protein (GRP75), a molecular chaperone, links ER and mitochondria by connecting the IP₃R with voltage-dependent anion channels (VDACs) [24]. Thus, we hypothesized that ER-mitochondria linkage proteins could alter the response of cells to Ang II treatment. Interestingly, Ang II exposure for 72 h significantly decreased GRP75 and Mfn-2 levels ($P < 0.01$ vs. control), and SA4503 treatment rescued this effect ($P < 0.01$ vs. Ang II) (Fig. 4B). Treatment with NE-100 combined with SA4503 totally abolished the SA4503 effect ($P < 0.01$ vs. SA) (Fig. 4B). Unexpectedly, expression of other mitochondria-associated proteins, namely Mfn-1 and VDAC, was not altered after Ang II exposure for 72 h, suggesting that mitochondria are not significantly degraded after Ang II exposure and that SA4503-induced rescue of ATP production correlates with alterations in ER-mitochondrial linkage proteins.

3.5. The effect of sigma-1 receptor stimulation by SA4503 on myocardial hypertrophy and dysfunction

To assess potential SA4503-mediated cardioprotective and antihypertrophic effects in vivo, we administered either SA4503 alone or SA4503 combined with NE-100 orally to TAC mice for 4 weeks, starting at TAC onset. One-way ANOVA analysis showed a significant

group effect on LV fractional shortening (%) [F (5, 47) = 4.747, $P < 0.01$] and left ventricular end-systolic diameter (LVESD) [F (5, 47) = 4.169, $P < 0.01$] in vivo. Post hoc analysis showed that TAC treatment significantly decreased LV fractional shortening and increased LVESD ($P < 0.01$ vs. sham) compared with sham-operated mice (Fig. 5A, B and C), consistent with our previous report [6]. SA4503 treatment restored decreased LV fractional shortening ($P < 0.05$ vs. TAC-vehicle for SA 0.3 and $P < 0.01$ vs. TAC-vehicle for SA 1.0) (Fig. 5A and B) and increased LVESD dose-dependently ($P < 0.05$ vs. TAC-vehicle for SA 1.0) (Fig. 5A and C). Co-administration of NE-100 abolished SA4503-mediated amelioration of heart dysfunction, as indicated by decreased LV fractional shortening (FS%) and increased LVESD ($P < 0.01$ vs. SA 1.0) (Fig. 5A, B and C). These results suggest that SA4503 ameliorates cardiac contractile dysfunction through activation of the σ_1 R.

Similarly, one-way ANOVA analysis showed a significant group effect on HW-to-BW [F (5, 23) = 21.266, $P < 0.01$] and LW-to-BW [F (5, 23) = 15.610, $P < 0.01$] ratios in vivo. Post hoc analysis showed that SA4503 treatment significantly restored the HW-to-BW ratio ($P < 0.01$ vs. TAC-vehicle for SA 0.3 and SA 1.0) (Fig. 5D) and the LW-to-BW ratio ($P < 0.01$ vs. TAC-vehicle for SA 0.3 and SA 1.0) dose-dependently (Fig. 5B). Co-administration of NE-100 abolished SA4503 inhibition of TAC-induced hypertrophy, as indicated by HW-to-BW ($P < 0.05$ vs. sham; $P < 0.01$ vs. SA 1.0) (Fig. 5D) and LW-to-BW ($P < 0.05$ vs. sham; $P < 0.01$ vs. SA 1.0) ratios (Fig. 5E). Taken together, we conclude that the anti-pathological hypertrophic effect of SA4503 on TAC mice is mediated by σ_1 R stimulation in vivo.

3.6. Effect of SA4503 treatment on σ_1 R and IP₃R2 expression in TAC mice

We previously documented that the σ_1 R is down-regulated concomitant with increased contractile dysfunction in TAC mice 4 weeks after TAC and that flvoxamine treatment rescued σ_1 R expression [6]. We confirmed SA4503 effects on σ_1 R levels. One-way ANOVA analysis showed a significant group effect on σ_1 R [F (5, 33) = 12.322, $P < 0.01$] and IP₃R2 [F (5, 32) = 3.033, $P < 0.05$] expression in vivo. As expected, SA4503 treatment significantly and dose-dependently restored σ_1 R levels ($P < 0.05$ vs. TAC-vehicle for SA 0.3 and $P < 0.01$ vs. TAC-vehicle for SA 1.0) (Fig. 6A, B). By contrast, TAC-induced hypertrophy was associated with increased IP₃R2 expression levels in the LV ($P < 0.01$ vs. sham). SA4503 administration significantly and dose-dependently decreased hypertrophy ($P < 0.01$ vs. TAC-vehicle for SA 1.0) (Fig. 6A, C). Although co-administration of NE-100 with SA4503 abolished SA4503-mediated cardioprotective effects (Fig. 5), co-administration of NE-100 did not abolish SA4503-mediated increases in σ_1 R expression ($P < 0.01$ vs. TAC-vehicle) in the LV (Fig. 6A, B). On the other hand, co-administration of NE-100 with SA4503 totally abolished SA4503-mediated decreases in IP₃R2 expression (Fig. 6A, C). These results suggested that SA4503-induced restoration of imbalance between σ_1 R and IP₃R2 levels is correlated with its cardioprotective activity in animals subjected to TAC-induced cardiac pathological hypertrophy and dysfunction.

3.7. σ_1 R stimulation increases ATP content in TAC mice

Our in vitro studies of cardiomyocytes clearly demonstrate that stimulation of the σ_1 R and subsequently of the IP₃R by SA4503 is critical for ATP production (Fig. 3). Thus, we confirmed the effects of SA4503 on ATP production in the LV of TAC mice. One-way ANOVA analysis showed a significant group effect on ATP content [F (5, 47) = 7.809,

Fig. 3. Intracellular localization of σ_1 R and ATP content following treatment with Ang II and SA4503. A, cultured cardiomyocytes were processed using immunofluorescence to mark the σ_1 R (green) and MitoTracker Red CMXRos (red) to mark mitochondria. Scale bar = 8 μ m. B, measurement of cellular ATP content 72 h after treatment with 100 nM Ang II with or without SA4503 treatment for the last 24 h. Each group consists of 4 samples. C, measurement of cellular ATP content with or without 10 μ M PE stimulation. Each group consists of 4 samples. Data are expressed as percentages of the control cell value (mean \pm S.E.M.) *, $P < 0.05$ and **, $P < 0.01$ versus control cells; ##, $P < 0.01$ versus Ang II-treated cells; †, $P < 0.05$ and ††, $P < 0.01$ versus Ang II plus 1 μ M SA4503-treated cells; ‡‡, $P < 0.01$ versus the non-stimulated cells. NE: NE-100 (10 μ M for 24 h). Xest: Xestospingon C (1 μ M for 24 h).

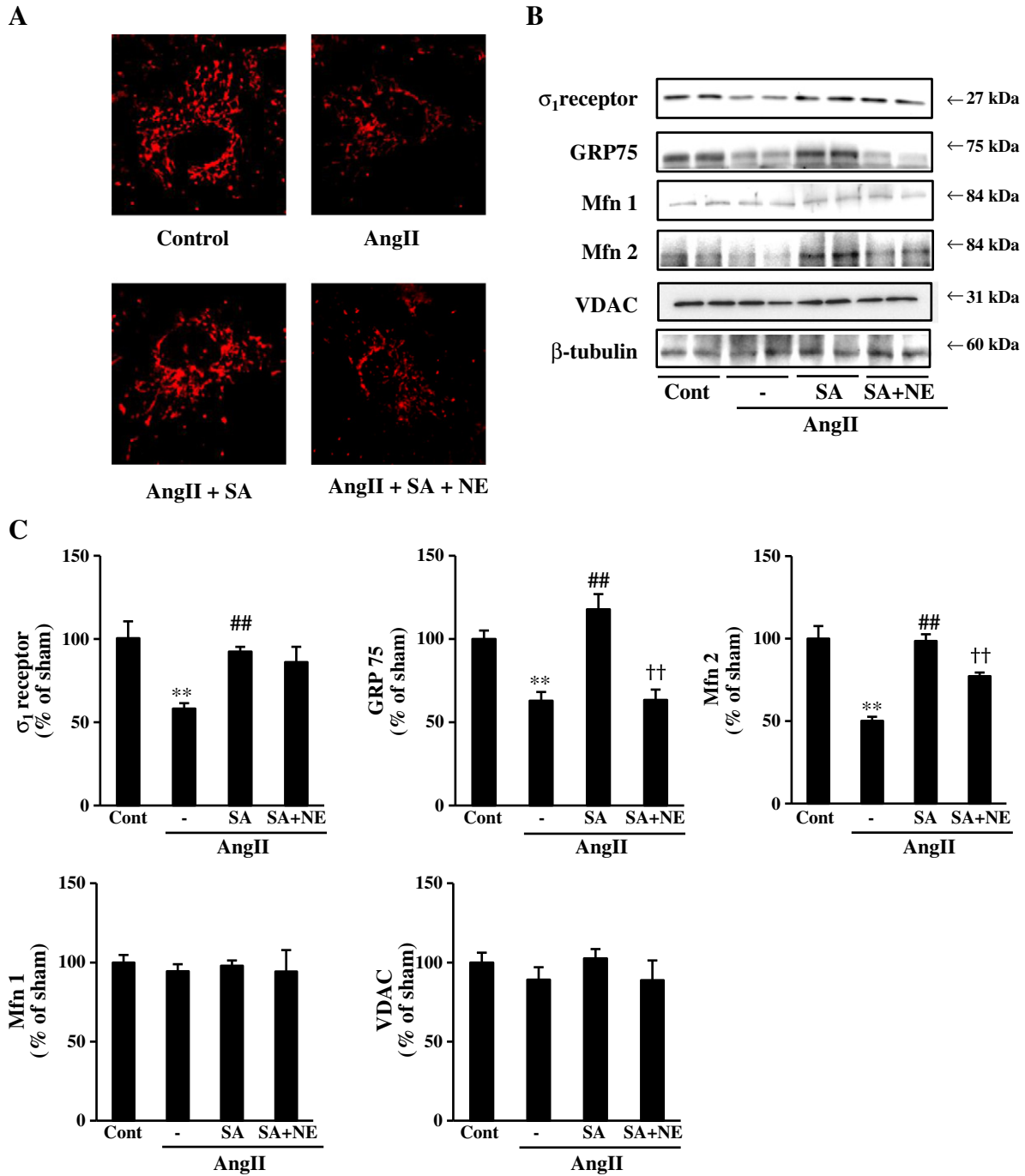


Fig. 4. Effect of SA4503 and NE-100 on expression of σ_1 R and ER-mitochondria junctional proteins. A, cultured cardiomyocytes were processed using immunofluorescence to monitor mitochondrial morphology using Cytochrome c (red). Scale bar = 15 μ m. B, western blot analysis of σ_1 R, VDAC and ER-mitochondria junctional protein expression in neonatal rat ventricular myocytes with or without drug treatment. Immunoblotting with anti- β -tubulin antibody indicates equal protein loading in each lane. C, densitometric quantification of σ_1 R and VDAC immunoreactive bands. Each group consists of 4 samples. Data are expressed as percentages of control cell values (mean \pm S.E.M.) **, $P < 0.01$ versus control cells; ##, $P < 0.01$ versus Ang II-treated cells; ††, $P < 0.01$ versus Ang II plus 1 μ M SA4503-treated cells.

$P < 0.01$] in vivo. Post hoc analysis showed that ATP content of the TAC mouse LV was significantly decreased compared to sham mice ($P < 0.05$ vs. sham) (Fig. 6D). SA4503 treatment (0.3, 1.0 mg/kg) significantly and completely ameliorated reduced ATP content dose-dependently ($P < 0.05$ vs. TAC for SA 0.3 and SA 1.0) (Fig. 6D), and an effect completely abolished in the presence of NE-100 (Fig. 6D). These observations strongly suggest that SA4503-mediated increases in ATP content are mediated by the σ_1 R and that these activities underlie its cardioprotective effects.

4. Discussion

The present study addresses how σ_1 R stimulation ameliorates cardiac hypertrophy and dysfunction in vitro and in vivo. We first defined effects of SA4503, a selective σ_1 R agonist, on IP_3 -mediated Ca^{2+} mobilization into mitochondria and on ATP production. We also focused on the effects of SA4503 on mitochondrial damage caused by oxidative stress following Ang II-induced hypertrophy in cardiomyocytes. Hayashi and Su [12] have proposed an attractive

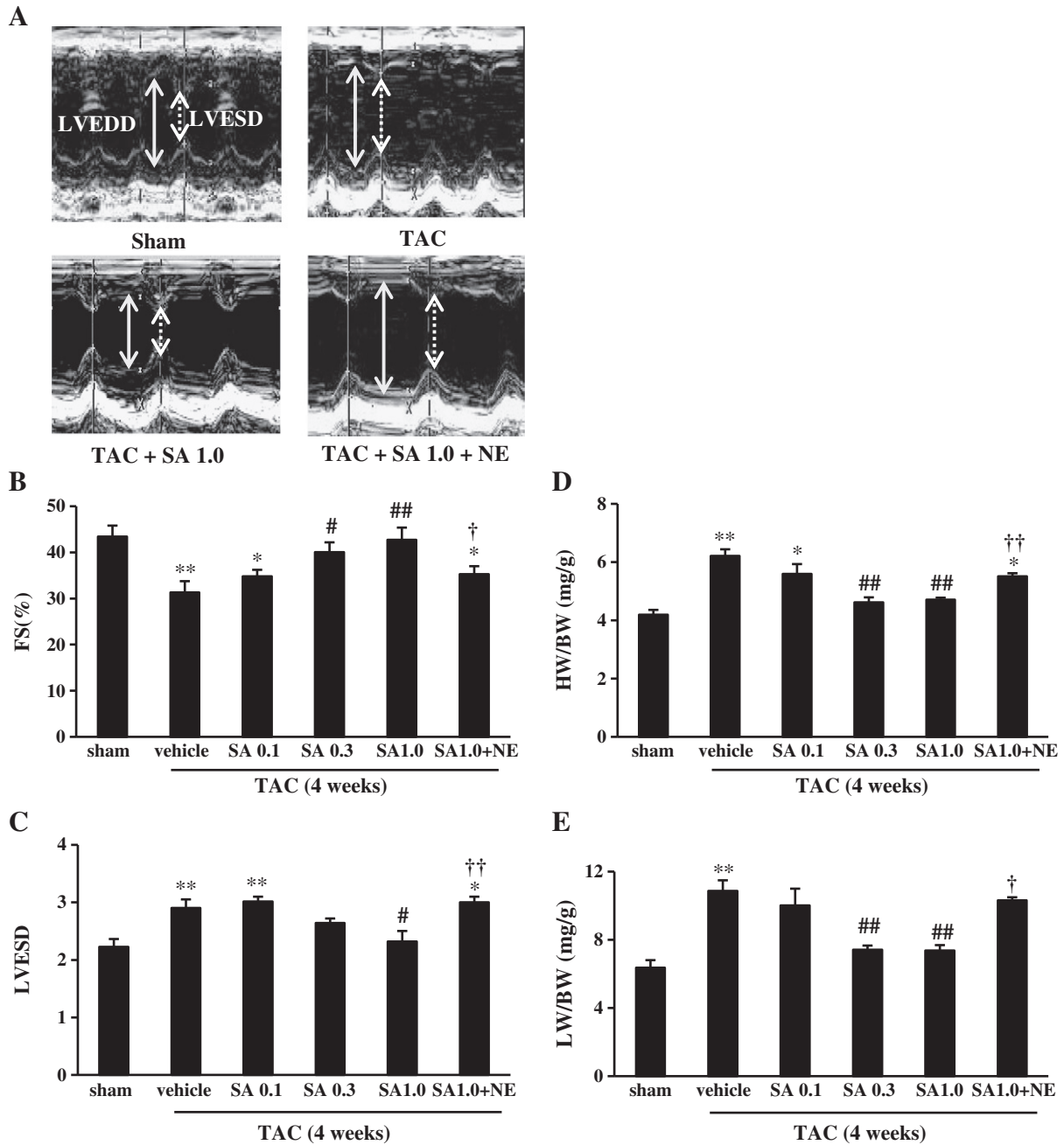


Fig. 5. Effect of SA4503 and NE-100 on cardiac failure and hypertrophy induced by TAC. A, representative M-mode echocardiograms of mice with or without SA4503 and/or NE-100 treatments. B, changes in percentage of LV fractional shortening (FS%). C, changes of left ventricular end-systolic diameter (LVESD). TAC mice were treated with SA4503 (0.1, 0.5 or 1.0 mg/kg) or SA4503 (1.0 mg/kg) plus NE-100 (1.0 mg/kg) as indicated. D, TAC-induced cardiac hypertrophy as indicated by the heart weight/body weight (HW/BW) ratio. E, TAC-induced cardiac hypertrophy as indicated by the lung weight/body weight (LW/BW) ratio. Each group consists of 4–5 mice. Data are expressed as percentages of values of sham-operated animals (mean \pm S.E.M.). *, $P < 0.05$ and **, $P < 0.01$ versus the sham group; #, $P < 0.05$ and ##, $P < 0.01$ versus the TAC/vehicle treated group; †, $P < 0.05$ and ††, $P < 0.01$ versus the TAC plus SA4503 (1 mg/kg)-treated group.

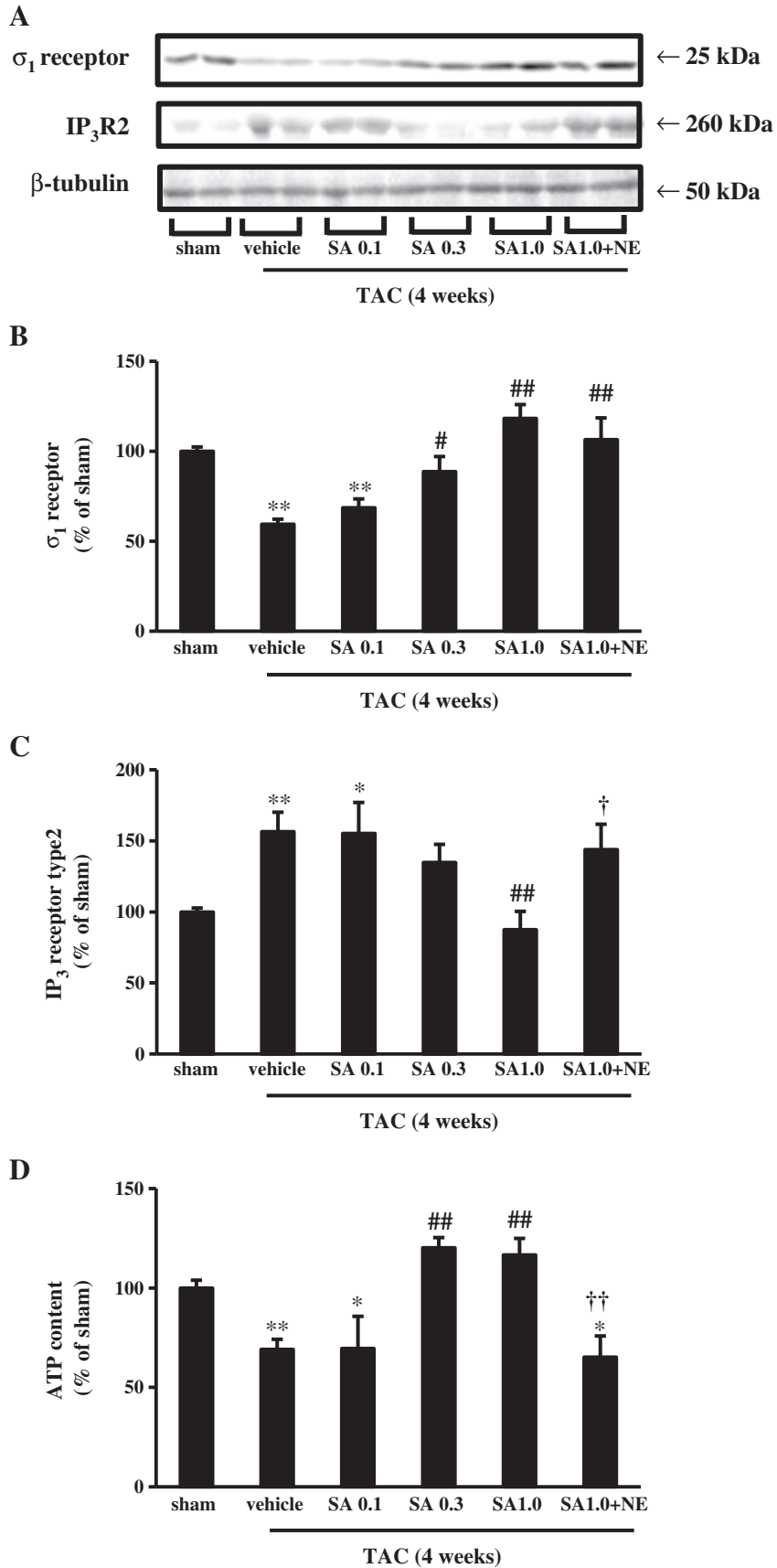
model that the σ_1 R supports cell survival via interaction with the IP_3R3 , allowing Ca^{2+} entry into mitochondria in CHO cells. Our results further strengthen the evidence that the Ca^{2+} entry into mitochondria through σ_1R/IP_3R complex promotes ATP production in cardiomyocytes.

One of the striking observations shown here is that prolonged (72 h) exposure to Ang II decreases ATP content and promotes mitochondrial fission and/or degradation, suggesting that mitochondrial dysfunction occurs when cardiac hypertrophy progresses to heart failure. Indeed, mitochondrial fission or degeneration was observed in H9c2 and HL-1

cardiac cells in ischemic conditions and, interestingly, pharmacological inhibition of mitochondrial fission reportedly protects cardiomyocytes from ischemia-induced apoptosis [25,26]. These observations suggest that mitochondrial fission or degradation triggers apoptosis or mitophagy associated with mitochondrial energy depletion [27]. Mitochondrial fission or degeneration was also observed in mice doubly-deficient in mitofusin-1 and -2, mitochondrial dynamin-related proteins that promote fusion, and these mice showed LV fractional shortening by 2 weeks of age [28]. Notably, we found that SA4503 treatment during the last 24 h of 72 h Ang II exposure totally rescued reduced ATP content

in hypertrophic cardiomyocytes concomitant with reduced hypertrophy. Since increased ATP consumption could continue after Ang II exposure, we also defined PE-induced ATP production which was totally abolished

Ru360, a specific inhibitor of mitochondrial calcium uptake. Prolonged (24 h) SA4503 treatment restored reduced ATP content in vitro and in vivo. Moreover, SA4503 rescued impaired PE-induced ATP production



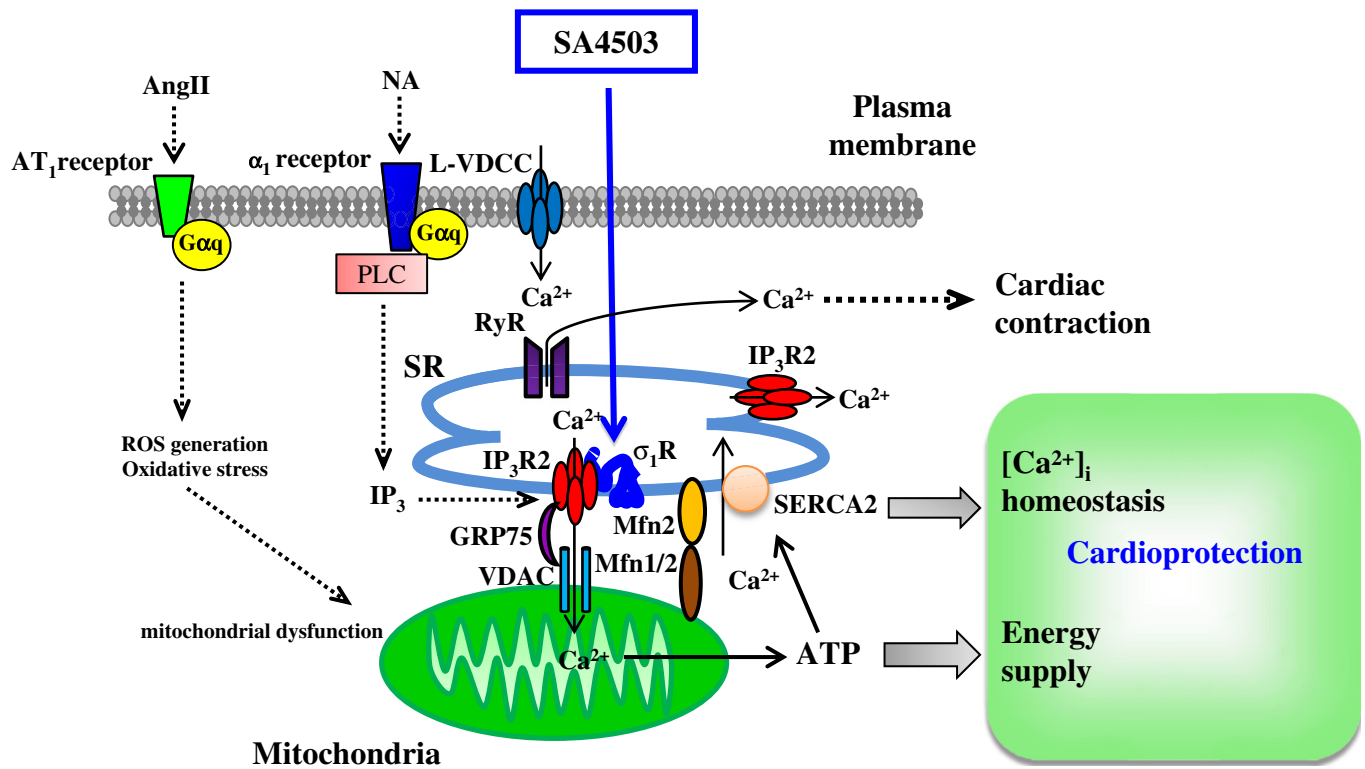


Fig. 7. Schematic representation of the hypothesis tested and results obtained. Shown is a model of regulation of $[Ca^{2+}]_i$ homeostasis and ATP production by SA4503 through σ_1R stimulation, as suggested by findings presented here. σ_1R stimulation with SA4503 promotes mitochondrial Ca^{2+} influx and mitochondrial Ca^{2+} -dependent ATP production. Increasing ATP production ameliorates sarco/endoplasmic reticulum Ca^{2+} -ATPase (SERCA2) activity, preventing SR Ca^{2+} depletion and increasing the cardiomyocyte energy supply. σ_1R -induced regulation of $[Ca^{2+}]_i$ homeostasis and ATP production is crucial for the cardioprotective activity of SA4503 against heart failure. VDAC: voltage-dependent anion channel.

in cultured cardiomyocytes, an effect closely associated with mitochondrial elongation (Fig. 3A). Importantly, we recently reported that σ_1R over-expression in neuro2A cells promotes mitochondrial elongation and IP₃R-dependent ATP production [29]. Taken together, SA4503 treatments likely promote mitochondrial elongation and stabilization of the IP₃R in SR membranes of cardiomyocytes, enhancing Ca^{2+} mobilization into mitochondria.

We also speculated that σ_1R stimulation at the mitochondrial ER-membrane enhances Ca^{2+} transport from the ER into mitochondria, thereby activating the tricarboxylic acid (TCA) cycle. Two hertz electrical stimulation of adult rat cardiomyocytes enhances mitochondrial Ca^{2+} influx, increasing mitochondrial ATP content [30]. Denton and McCormack also showed that activities of glycerophosphate dehydrogenase, pyruvate dehydrogenase, isocitrate dehydrogenase, and oxoglutarate dehydrogenase, which are mitochondrial and mitochondrial matrix dehydrogenase enzymes functioning in the TCA cycle, are regulated by mitochondrial Ca^{2+} concentration [31–34]. We first confirmed that SA4503 treatment rescues PE-induced Ca^{2+} mobilization into mitochondria (Fig. 2A). Notably, in control cells PE elicited biphasic mitochondrial Ca^{2+} mobilization, likely due to IP₃R-mediated transient and store- or voltage-operated persistent Ca^{2+} mobilization in cardiomyocytes. Interestingly, SA4503 had a prominent effect on IP₃R-mediated transient Ca^{2+} mobilization without altering persistent Ca^{2+} mobilization, suggesting that SA4503 rescues IP₃R-mediated mitochondrial Ca^{2+} mobilization. More importantly, SA4503 slightly but significantly enhanced cytosolic Ca^{2+} mobilization

by PE. Thus, the σ_1R is critical to regulate IP₃R-mediated mitochondrial Ca^{2+} mobilization. Furthermore, mitochondrial elongation observed following SA4503 treatment also likely plays a crucial role in IP₃R-mediated mitochondrial Ca^{2+} mobilization.

Chronic Ang II exposure caused Ca^{2+} overload in the cytosol [35]. In particular, ryanodine receptors (RyRs) are major Ca^{2+} -releasing channels in cardiac myocytes. We examined the role of RyRs on mitochondrial Ca^{2+} uptake. Treatment of cultured cardiomyocytes with ryanodine, which opens the RyR channel, induced Ca^{2+} release into the cytosol (Supplemental Fig. 1A), but failed to increase mitochondrial Ca^{2+} influx (Supplemental Fig. 1B). These data suggested that the RyR does not directly regulate mitochondrial Ca^{2+} influx.

Recent studies reveal that specific proteins and chaperones function as ER-mitochondria linkage proteins. For example, mitofusin-2 not only connects mitochondria but also bridges the ER and mitochondria and functions in IP₃-induced mitochondrial Ca^{2+} uptake [23]. Moreover, Szabadkai et al. report that glucose-regulated protein (GRP75), a molecular chaperone, links the ER and mitochondria by connecting the IP₃R with voltage-dependent anion channels (VDACs) [24]. Mitofusin-2 is localized in both ER and mitochondrial membranes, whereas GRP75 and mitofusin-1 are predominantly localized to the mitochondrial membrane. Here, we found, for the first time, that σ_1R downregulation is associated with reduction in levels of the junctional proteins mitofusin-2 and GRP 75. Notably, levels of mitofusin-1 and VDAC were unchanged after Ang II-induced mitochondrial fission, suggesting that Ang II

Fig. 6. Effects of SA4503 and NE-100 on σ_1R and IP₃R2 expression and ATP content in TAC mice. A western blot analysis of σ_1R , IP₃R2 and β -tubulin (as a loading control) expression in the LV of sham and TAC-mice with or without drug treatment. Immunoblotting with anti- β -tubulin antibody indicates equal protein loading in each lane. B, densitometric quantification of σ_1R immunoreactive bands. C, densitometric quantification of IP₃R2 immunoreactive bands. D, measurement of cellular ATP content in the LV of TAC mice with or without drug treatment. Each group consists of 4–5 mice. Data are expressed as percentages of values of sham-operated animals (mean \pm S.E.M.). *, $P < 0.05$ and **, $P < 0.01$ versus the sham group; #, $P < 0.05$ and ##, $P < 0.01$ versus the TAC/vehicle-treated group; †, $P < 0.05$ and ††, $P < 0.01$ versus the TAC plus SA4503 (1 mg/kg)-treated group.

treatment, at least for 72 h, has no apparent effect of mitophagy or mitochondrial breakdown. σ_1 R agonists likely rescue mitochondrial fission by stabilizing GRP75 and mitofusin-2, although further studies are required to identify mechanisms underlying this effect.

Overall, chronic Ang II exposure causes mitochondrial dysfunction via oxidative stress. Previous studies conducted in various cell lines suggest that Ang II induces oxidative stress by stimulating NADPH oxidase-derived superoxide generation, promoting mitochondrial dysfunction [36,37]. Another report suggests that calcineurin dephosphorylates dynamin-related protein (Drp) 1, a key regulator of mitochondrial fission, promoting mitochondrial fission [38]. Further studies are required to identify mechanisms underlying mitochondrial fission and how they are regulated by the σ_1 R.

Ito et al. [11] have reported that pressure overload and high-salt diet-induced heart failure mice exhibit reduced σ_1 R levels in the brain, with concomitant depression-like behavior. Chronic infusion in those model mice with PRE084, a σ_1 R agonist, significantly reduced sympathetic nerve activation. These authors conclude that suppression of sympathetic nerve activation by a σ_1 R agonist acting in the brain improves heart function in pressure overload mice. We observed that xestospingonin C treatment abolished increased ATP content mediated by SA4503 and antagonized amelioration of cardiomyocyte hypertrophy by SA4503. This finding supports our hypothesis that SA4503 directly stimulates the σ_1 R in cardiomyocytes, rescuing IP₃R-mediated ATP production and cardiac dysfunction. We propose that both indirect and direct mechanisms through the σ_1 R underlie cardioprotection seen in TAC mice.

5. Conclusions

For the first time, we provide evidence that SA4503, a potent and selective σ_1 R agonist, ameliorates TAC-induced cardiac hypertrophy and dysfunction by activating the σ_1 R. Rescue of IP₃R-mediated mitochondrial Ca²⁺ transport and ATP production following SA4503 treatment was critical to maintain the energy supply and [Ca²⁺]_i homeostasis required for proper cardiac contraction and relaxation (Fig. 7). We also report that signaling through the σ_1 R counteracts Ang II-induced cardiac myocyte apoptosis by rescuing SR-mitochondria calcium mobilization and mitochondrial ATP production. Indeed, the effect of SA4503 treatment has recently been tested in humans in a stroke and depression clinical phase II trial (NCT00639249). Our observations suggest a new therapeutic strategy to rescue the heart from hypertrophic dysfunction via σ_1 R stimulation.

Supplementary data to this article can be found online at <http://dx.doi.org/10.1016/j.bbagen.2012.12.029>.

Conflict of interest statement

The authors declare that there are no conflicts of interest.

Acknowledgments

This work was supported in part by grants-in-aid for Scientific Research from the Ministry of Education, Science, Sports and Culture of Japan (22390109 to K.F.).

References

- C.B. Taylor, M.E. Youngblood, D. Catellier, R.C. Veith, R.M. Carney, M.M. Burg, P.G. Kaufmann, J. Shuster, T. Mellman, J.A. Blumenthal, R. Krishnan, A.S. Jaffe, ENRICH Investigators, Effects of antidepressant medication on morbidity and mortality in depressed patients after myocardial infarction, *Arch. Gen. Psychiatry* 62 (7) (2005) 792–798.
- A. Schmidt, L. Lebel, B.K. Koe, T. Seeger, J. Heym, Sertraline potently displaces (+)-[3H] 3-PPP binding to sigma sites in rat brain, *Eur. J. Pharmacol.* 165 (1989) 335–336.
- M. Ishikawa, K. Ishiwata, K. Ishii, Y. Kimura, M. Sakata, M. Naganawa, K. Oda, R. Miyatake, M. Fujisaki, E. Shimizu, Y. Shirayama, M. Iyo, K. Hashimoto, High occupancy of sigma-1 receptors in the human brain after single oral administration of fluvoxamine: a positron emission tomography study using [¹¹C]SA4503, *Biol. Psychiatry* 62 (2007) 878–883.
- C. Ela, J. Barg, Z. Vogel, Y. Hasin, Y. Eilam, Sigma receptor ligands modulate contractility, Ca²⁺ influx and beating rate in cultured cardiac myocytes, *J. Pharmacol. Exp. Ther.* 269 (1994) 1300–1309.
- M.S. Bhuiyan, H. Tagashira, K. Fukunaga, Targeting sigma-1 receptor with fluvoxamine ameliorates pressure-overload-induced hypertrophy and dysfunctions, *Expert Opin. Ther. Targets* 14 (10) (2010) 1009–1022.
- H. Tagashira, M.S. Bhuiyan, N. Shioda, H. Hasegawa, H. Kanai, K. Fukunaga, Sigma-1 receptor stimulation with fluvoxamine ameliorates transverse aortic constriction-induced myocardial hypertrophy and dysfunction in mice, *Am. J. Physiol. Heart Circ. Physiol.* 299 (5) (2010) H1535–H1545.
- M.S. Bhuiyan, K. Fukunaga, Stimulation of sigma-1 receptor signaling by dehydroepiandrosterone ameliorates pressure overload-induced hypertrophy and dysfunctions in ovariectomized rats, *Expert Opin. Ther. Targets* 13 (2009) 1253–1265.
- H. Tagashira, M.S. Bhuiyan, N. Shioda, K. Fukunaga, Distinct cardioprotective effects of 17 β -estradiol and dehydroepiandrosterone on pressure-overload-induced hypertrophy in ovariectomized female rats, *Menopause* 18 (12) (2011) 1317–1326.
- M.S. Bhuiyan, H. Tagashira, K. Fukunaga, Dehydroepiandrosterone mediated stimulation of sigma-1 receptor activates Akt-eNOS signaling in the thoracic aorta of ovariectomized rats with abdominal aortic banding, *Cardiovasc. Ther.* 29 (4) (2011) 219–230.
- M.S. Bhuiyan, H. Tagashira, K. Fukunaga, Sigma-1 receptor stimulation with fluvoxamine activates Akt-eNOS signaling in the thoracic aorta of ovariectomized rats with abdominal aortic banding, *Eur. J. Pharmacol.* 650 (2–3) (2011) 621–628.
- K. Ito, Y. Hirooka, R. Matsukawa, M. Nakano, K. Sunagawa, Decreased brain sigma-1 receptor contributes to the relationship between heart failure and depression, *Cardiovasc. Res.* 93 (1) (2012) 33–40.
- T. Hayashi, T.P. Su, Sigma-1 receptor chaperones at the ER-mitochondrion interface regulate Ca²⁺ signaling and cell survival, *Cell* 131 (2007) 596–610.
- D.J. Bare, C.S. Kettlun, M. Liang, D.M. Bers, G.A. Mignery, Cardiac type 2 inositol 1,4,5-trisphosphate receptor: interaction and modulation by calcium/calmodulin-dependent protein kinase II, *J. Biol. Chem.* 280 (2005) 15912–15920.
- X. Li, A.V. Zima, F. Sheikh, L.A. Blatter, J. Chen, Endothelin-1-induced arrhythmogenic Ca²⁺ signaling is abolished in atrial myocytes of inositol-1,4,5-trisphosphate (IP₃)-receptor type 2-deficient mice, *Circ. Res.* 96 (2005) 1274–1281.
- T. Uchiyama, F. Yoshikawa, A. Hishida, T. Furuichi, K. Mikoshiba, A novel recombinant hyperaffinity inositol 1,4,5-trisphosphate (IP₃) absorbent traps IP₃, resulting in specific inhibition of IP₃-mediated calcium signaling, *J. Biol. Chem.* 277 (10) (2002) 8106–8113.
- H. Nakayama, I. Bodi, M. Maillet, J. DeSantiago, T.L. Domeier, K. Mikoshiba, J.N. Lorenz, L.A. Blatter, D.M. Bers, J.D. Molkenstein, The IP₃ receptor regulates cardiac hypertrophy in response to select stimuli, *Circ. Res.* 107 (5) (2010) 659–666.
- K. Fujimura, J. Matsumoto, M. Niwa, T. Kobayashi, Y. Kawashima, Y. In, T. Ishida, Synthesis, structure and quantitative structure-activity relationships of sigma receptor ligands, 1-[2-(3,4-dimethoxyphenyl)ethyl]-4-(3-phenylpropyl) piperazines, *Bioorg. Med. Chem.* 5 (8) (1997) 1675–1683.
- Y.M. Lu, F. Han, N. Shioda, S. Moriguchi, Y. Shirasaki, Z.H. Qin, K. Fukunaga, Phenylephrine-induced cardiomyocyte injury is triggered by superoxide generation through uncoupled endothelial nitric-oxide synthase and ameliorated by 3-[2-[4-(3-chloro-2-methylphenyl)-1-piperazinyl]ethyl]-5,6-dimethoxyindazole (DY-9836), a novel calmodulin antagonist, *Mol. Pharmacol.* 75 (1) (2009) 101–112.
- M.S. Bhuiyan, N. Shioda, M. Shibuya, Y. Iwabuchi, K. Fukunaga, Activation of endothelial nitric oxide synthase by a vanadium compound ameliorates pressure overload-induced cardiac injury in ovariectomized rats, *Hypertension* 53 (1) (2009) 57–63.
- Y.M. Lu, N. Shioda, F. Han, S. Moriguchi, J. Kasahara, Y. Shirasaki, Z.H. Qin, K. Fukunaga, Imbalance between CaM kinase II and calcineurin activities impairs caffeine-induced calcium release in hypertrophic cardiomyocytes, *Biochem. Pharmacol.* 74 (12) (2007) 1727–1737.
- R.A. Bassani, J.W. Bassani, D.M. Bers, Mitochondrial and sarcolemmal Ca²⁺ transport reduce [Ca²⁺]_i during caffeine contractures in rabbit cardiac myocytes, *J. Physiol.* 453 (1992) 591–608.
- W. Pendergrass, N. Wolf, M. Poot, Efficacy of MitoTracker Green and CMXRosamine to measure changes in mitochondrial membrane potentials in living cells and tissues, *Cytometry A* 61 (2) (2004) 162–169.
- O.M. de Brito, L. Scorrano, Mitofusin 2 tethers endoplasmic reticulum to mitochondria, *Nature* 456 (7222) (2008) 605–610.
- G. Szabadkai, K. Bianchi, P. Várnai, D. De Stefani, M.R. Wieckowski, D. Cavagna, A.I. Nagy, T. Balla, R. Rizzuto, Chaperone-mediated coupling of endoplasmic reticulum and mitochondrial Ca²⁺ channels, *J. Cell. Biol.* 175 (6) (2006) 901–911.
- L. Chen, Q. Gong, J.P. Stice, A.A. Knowlton, Mitochondrial OPA1, apoptosis, and heart failure, *Cardiovasc. Res.* 84 (1) (2009) 91–99.
- S.B. Ong, S. Subrayan, S.Y. Lim, D.M. Yellon, S.M. Davidson, D.J. Hausenloy, Inhibiting mitochondrial fission protects the heart against ischemia/reperfusion injury, *Circulation* 121 (18) (2010) 2012–2022.
- L.C. Gomes, G. Di Benedetto, L. Scorrano, During autophagy mitochondria elongate, are spared from degradation and sustain cell viability, *Nat. Cell. Biol.* 13 (5) (2011) 589–598.
- Y. Chen, Y. Liu, G.W. Dorn II, Mitochondrial fusion is essential for organelle function and cardiac homeostasis, *Circ. Res.* 109 (12) (2011) 1327–1331.
- N. Shioda, K. Ishikawa, H. Tagashira, T. Ishizuka, H. Yawo, K. Fukunaga, Expression of a truncated form of the endoplasmic reticulum chaperone protein, sigma-1 receptor, promotes mitochondrial energy depletion and apoptosis, *J. Biol. Chem.* 287 (28) (2012) 23318–23331.

- [30] C.J. Bell, N.A. Bright, G.A. Rutter, E.J. Griffiths, ATP regulation in adult rat cardiomyocytes: time-resolved decoding of rapid mitochondrial calcium spiking imaged with targeted photoproteins, *J. Biol. Chem.* 281 (38) (2006) 28058–28067.
- [31] R.G. Hansford, J.B. Chappell, The effect of Ca^{2+} on the oxidation of phosphate by blow-fly flight-muscle mitochondria, *Biochem. Biophys. Res. Commun.* 27 (1967) 686–692.
- [32] R.M. Denton, P.J. Randle, B.R. Martin, Stimulation by calcium ions of pyruvate dehydrogenase phosphate phosphatase, *Biochem. J.* 128 (1972) 161–163.
- [33] R.M. Denton, D.A. Richards, J.G. Chin, Calcium ions and the regulation of NAD^{+} -linked isocitrate dehydrogenase from the mitochondria of rat heart and other tissues, *Biochem. J.* 176 (1978) 899–906.
- [34] J.G. McCormack, R.M. Denton, The effects of calcium ions and adenine nucleotides on the activity of pig heart 2-oxoglutarate dehydrogenase complex, *Biochem. J.* 180 (1979) 533–544.
- [35] I. Goldenberg, E. Grossman, K.A. Jacobson, V. Shneyvays, A. Shainberg, Angiotensin II-induced apoptosis in rat cardiomyocyte culture: a possible role of AT1 and AT2 receptors, *J. Hypertens.* 19 (9) (2001) 1681–1689.
- [36] E.M. de Cavanagh, M. Ferder, F. Inserra, L. Ferder, Angiotensin II, mitochondria, cytoskeletal, and extracellular matrix connections: an integrating viewpoint, *Am. J. Physiol. Heart Circ. Physiol.* 296 (3) (2009) H550–H558.
- [37] U. Rueckschloss, M.T. Quinn, J. Holtz, H. Morawietz, Dose-dependent regulation of NAD(P)^{H} oxidase expression by angiotensin II in human endothelial cells: protective effect of angiotensin II type 1 receptor blockade in patients with coronary artery disease, *Arterioscler. Thromb. Vasc. Biol.* 22 (11) (2002) 1845–1851.
- [38] G.M. Cereghetti, A. Stangherlin, O. Martins de Brito, C.R. Chang, C. Blackstone, P. Bernardi, L. Scorrano, Dephosphorylation by calcineurin regulates translocation of Drp1 to mitochondria, *Proc. Natl. Acad. Sci. U. S. A.* 105 (41) (2008) 15803–15808.